Journal of Electroceramics, 13, 733–738, 2004

Poisoning of Temperature Independent Resistive Oxygen Sensors by Sulfur Dioxide

FRANK RETTIG,[1,2] RALF MOOS[1,2,*] & CARSTEN PLOG[2]
[1] *University of Bayreuth*
[2] *DaimlerChrysler AG, Research and Technology, Dornier GmbH*

Submitted February 13, 2003; Revised October 31, 2003; Accepted November 3, 2003

Abstract. Sulfur dioxide strongly affects temperature independent resistive oxygen sensors of $SrTi_{1-x}Fe_xO_{3-\delta}$. Time dependent sensor deterioration was investigated for lanthanum doped $SrTi_{0.65}Fe_{0.35}O_{3-\delta}$ (STF35). Parameters were sulfur dioxide concentration, oxygen partial pressure, temperature, and sensor morphology. The sensor poisoning consists of two steps. At lower temperatures sulfur dioxide adsorption and sulfate ion formation at the grain surface is suggested. At higher temperatures the material decomposes into $SrSO_4$, iron depleted STF35, and Fe_2TiO_5.

Keywords: exhaust gas sensor, resistive oxygen sensor, sulfur poisoning, titanates, perovskites

1. Introduction

In the past decade resistive oxygen sensors based on titanates or other transition metal oxides were suggested by several authors for lambda control in automotive exhausts [1–6]. Recently, it has been reported on compositions with temperature independent resistance behavior (e.g. doped $SrTi_{1-x}Fe_xO_3 = STF$) [7-10]. In contrast to titania, no sensor based on the above-mentioned temperature independent compositions has been serialized. The major drawback is the sulfur oxide poisoning, which impedes long-term stability. Therefore, sulfur adsorbers [11, 12] were introduced, leading to long-term stable sensors in real exhaust gas [10]. The problem of sulfur oxide poisoning emerges also in catalytically active perovskites [13] and in mixed electronic ionic conductors [14], when the materials contain earth alkaline ions.

This contribution investigates the sulfur instability of STF, mainly via conductivity measurements. As a result, a brief qualitative defect chemical picture is evolved describing the steps during poisoning.

*To whom all correspondence should be addressed. E-mail: Ralf.Moos@Uni-Bayreuth.de

2. Sample Preparation and Experimental Setup

Lanthanum doped $SrTi_{0.65}Fe_{0.35}O_3$-powders (here abbreviated STF35) were prepared in mixed oxide technique. Pastes of these powders were screen-printed on alumina substrates and fired at 1100°C to a very porous sensitive film. A strontium-spinel layer between substrate and sensor film served as a diffusion barrier layer [10]. Four platinum thick-film electrodes were used. A more detailed description of powder and sensor preparation can be found in Ref. [10].

Some additional experiments were conducted on differently sintered lanthanum doped STF35-tapes, which were cast from the same powders. The size was similar to the compacts in Ref. [9]. The thickness, however, was only about 80 μm. The sintered tapes were affixed with a platinum paste on the conductor tracks of the transducers.

After sintering, the devices were heated in a tube furnace to operating temperature. The resistance was measured offset compensated by 4-wire technique with a digital mulitmeter (Keithley 196). The sensor temperature was determined by thermocouples.

At first, oxygen sensitivity was checked by applying different oxygen partial pressures to the sensor (oxygen/nitrogen mixtures). Thereafter, the temperature

independency was checked. All samples exhibited *p*-type conductivity obeying $R \propto pO_2^{-m}$, with $m \approx 0.23$ between 10^{-4} bar and 1 bar and in the range of 700 to 900°C. Temperature dependency could be neglected, as expected from Ref. [9, 10]. Then, sensors were kept at distinct temperature and distinct oxygen partial pressure for equilibration. Finally, different amounts of sulfur oxide (SO_2) were added to the gas.

3. Results

First of all, the time dependency of the sensor deterioration was investigated in detail. After equilibration at 600, 700, 800 or 900°C in 3.2% O_2/96.8% N_2, approximately 380 ppm SO_2 were added to the gas mixture.[1]

For better comparability, in Fig. 1 the resistance is plotted normalized to its value before SO_2 exposition. R_0 denotes the resistance of the sensor before exposing it to SO_2. The poisoning behavior at high temperatures (900°C, 800°C) is different from the behavior at low temperatures (600°C, 700°C). At 600 and 700°C, the resistance increases almost stepwise when SO_2 is added. After this first "step", the further resistance increase occurs very slowly. At higher temperatures (800°C, 900°C) a resistance step can also be seen, but it is partially overlapped by a very fast resistance increase, particularly at 900°C. After exposing the sample for 10 min at 900°C to the SO_2 enriched gas, the resistance has increased by a factor of about seven. As shown previously [10], sensors deteriorated like this loose both temperature independency and oxygen sensitivity. Their resistance increases by decades, the slope *m* diminishes below 0.2 and the conductivity becomes strongly thermally activated.

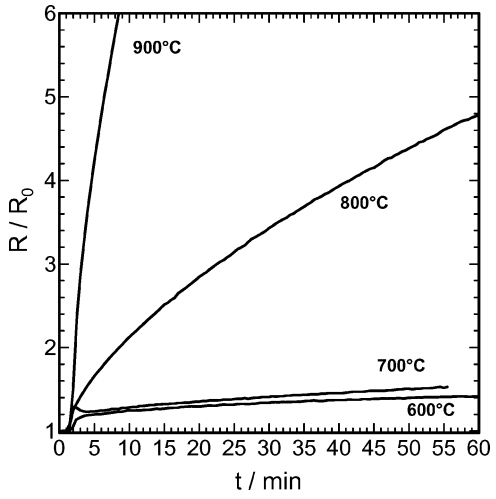

Fig. 1. Time dependent and normalized sensor resistance when exposed to 380 ppm SO_2 in 3.2% O_2/96.8% N_2. Parameter: sensor temperature. R_0 denotes the resistance of the sensor before exposing it to SO_2.

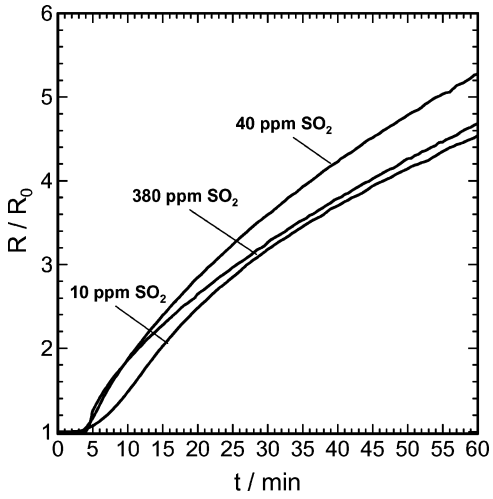

Fig. 2. Time dependent and normalized sensor resistance at 800°C when exposed to different SO_2 concentrations. Base line gas 3.2% O_2 / 96.8% N_2. R_0 denotes the resistance of the sensor before exposing it to SO_2.

These results imply the conclusion, that two different steps are responsible for the poisoning: A fast low temperature step that seems temperature independent and a high temperature step with strongly thermally activated kinetics.

Similar measurements were conducted on earth alkaline-free perovskites. $LaFeO_3$ sensors, exposed at 800°C to sulfur enriched O_2/N_2 mixtures also show a fast but small resistance step within the first two minutes [15]. However, in contrast to STF35, the resistance does not increase anymore after this first step.

XRD data of high temperature poisoned STF35 sensor samples were taken. Besides platinum (from the electrodes), strong $SrSO_4$-lines were found. In addition, weak lines of Fe_2TiO_5 (pseudo brookite) and of course cubic perovskite lines were observed. No other lines were found.

In a next work step, the resistance behavior due to different SO_2 concentrations was investigated. The sensors were equilibrated at 800°C with 3.2% O_2 in N_2. Then, 10 ppm SO_2, 40 ppm SO_2 or 380 ppm SO_2 were added.

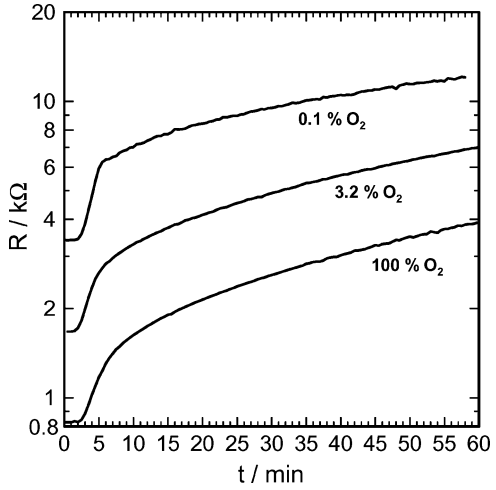

Fig. 3. Sensor deterioration at 800°C when exposed to 40 ppm SO_2. Parameter: oxygen concentration.

Not depending on the SO_2 concentration, almost the same time dependence of the resistance deterioration is found. It seems that the concentration of SO_2 does not have much influence on the poisoning velocity. Therefore, further experiments were conducted using 40 ppm SO_2.

In another experiment, sulfur poisoning was investigated at different oxygen partial pressures. The sensors were equilibrated at 800°C in 0.1, 3.2, and 100% oxygen, respectively. Then, 40 ppm SO_2 were added to the gas stream. Figure 3 shows the resulting time dependence of the resistance. In contrast to the previous figures, the ordinate is scaled logarithmically. In agreement with the $R \approx pO_2^{-m}$-behavior, at $t = 0$ when SO_2 exposition begins, the resistances exhibit different starting values. It is obvious that the more the oxygen concentration of the gas increases, the more the "first resistance step" becomes slower. The time dependency after the "first step" remains unchanged by the oxygen content of the gas.

The aforementioned results may lead to the assumption that the "first step" of the poisoning process is a surface phenomenon. Implying this, the morphology should strongly affect poisoning kinetics. Therefore, tapes of lanthanum doped STF35 were cast and sintered differently to obtain morphology variations. SEM-pictures of the surfaces are shown in Fig. 4.

Sample A was sintered at 1100°C for 1 h; it shows the largest porosity. Sample C, sintered for 10 h at 1300°C is almost dense and its surface is closed. Sample B (1200°C; 10 h) shows an intermediate porosity. Before poisoning experiments were started, oxygen sensitivity and temperature independency was verified. Tests with stepwise changed oxygen partial pressures (similarly to Ref. [9]) were conducted. Resistance response data were taken, leading to the time dependency of oxygen equilibration. As expected from theory of oxygen transport in titanates [16,17], the dense sample C showed the slowest equilibration kinetics. At 800°C six minutes per pO_2 step were not sufficient to completely equilibrate the dense sample C (thickness 80 μm). This was in strong contrast to the resistance of the porous sample A, which followed the pO_2-steps immediately. As expected from its morphology, sample B was faster than sample C and slower than sample A. These short dynamic tests were performed only to support additionally that the sensor morphology was varied by the different sintering procedures. Another evidence that porosity decreased with the

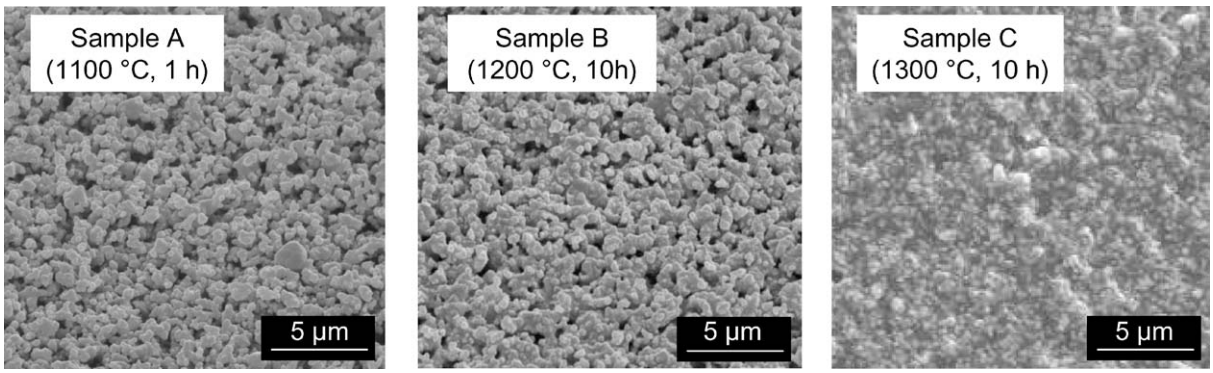

Fig. 4. Morphology of differently sintered tapes.

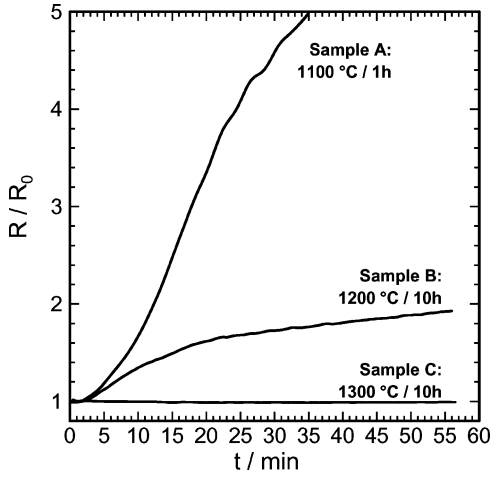

Fig. 5. Sensor deterioration at 800°C when exposed to 40 ppm SO_2. Samples from Fig. 4. R_0 denotes the resistance of the sensor before exposing it to SO_2.

sintering temperature was the absolute resistance value at $pO_2 \approx 1$ bar. Although the samples had almost the same geometry, their resistance decreased from 800 Ω (sample A) to 200 Ω (sample B) and 40 Ω (sample C).

After equilibration at 800°C in 3.2% O_2 (balance N_2), the three samples were exposed to 40 ppm SO_2. The result is shown in Fig. 5.

It is eye-catching that the dense sample C shows no deterioration, whereas sample A behaves as already known from Fig. 2. The sensor poisoning seems to be inhibited if SO_2 has only few sites to adhere. From a long-term stability point of view dense samples should be first choice, however, they are by far too slow for automotive exhaust gas applications. Figure 5 leads to the assumption that poisoning of these titanates starts at and is limited by the surface, the latter at least at lower temperatures.

4. Discussion

In this section, a brief qualitative model will be evolved that is able to explain mechanistically sulfur poisoning of the samples. It is developed from the results of the previous section. The model shall be considered as an initial thesis that needs to be confirmed by further experiments. Two different mechanisms appear to play a role in sensor poisoning. It is assumed that at lower temperature adsorption and sulfate formation occurs. At higher temperatures, STF35 decomposes thermally activated.

Figure 6 illustrates the processes that lead to the observed first "resistance step". It shows an Sr-O-plane that terminates the crystal surface. Titanium ions are

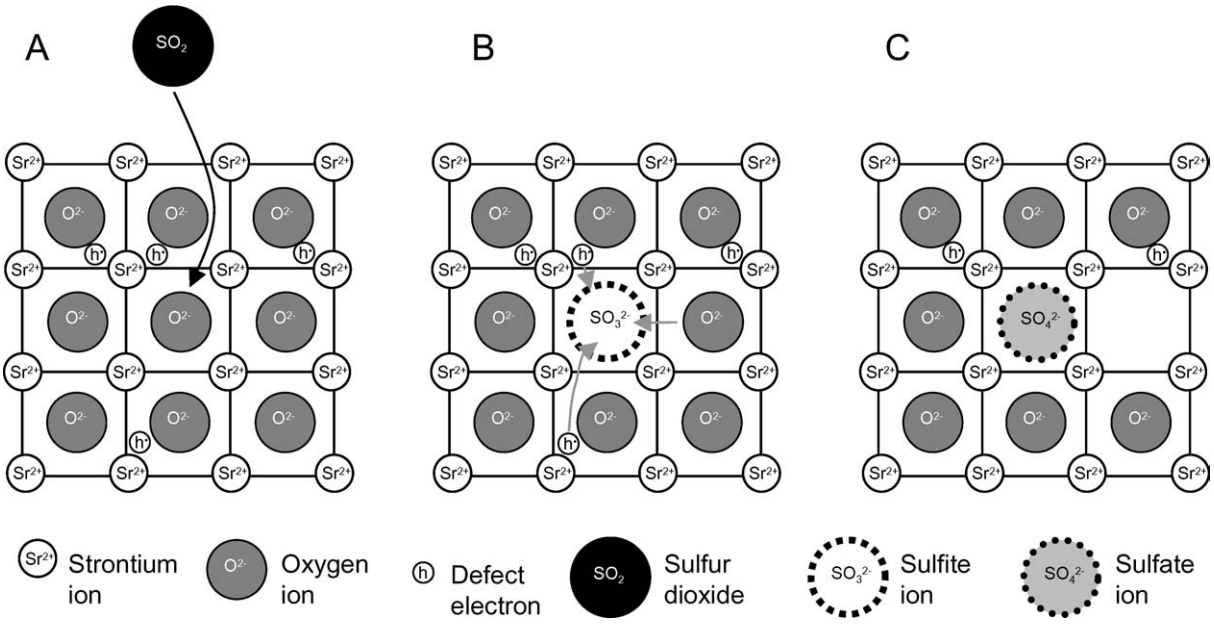

Fig. 6. SO_2 adsorption and sulfate formation in STF. Note: the defect electron concentration h^+ is reduced due to the reduction of the surface.

not sketched for the sake of clarity. As soon as the sensor material is exposed to SO_2, SO_2 adsorption on an oxygen site ($O^x_{O,surface}$) of the crystal surface starts (step A in Fig. 6).[2] Sulfite ions are formed directly on the grain boundary ($SO^x_{2O,surface}$) acc. to Eq. (1), (step B).

$$SO_2 + O^x_{O,surface} \rightarrow (SO_3)^x_{O,surface} \quad (1)$$

Since no charge carriers are involved in Eq. (1), the electrical conductivity of the samples should not be affected by steps A and B. According to the above-presented results, the fast "resistance step" is likely due to a grain boundary effect. Therefore, sulfate formation, Eq. (2), is assumed to occur next (step C). The formation of one sulfate ion consumes two defect electrons ($h^\bullet$) and a second surface oxygen ion.

$$(SO_3)^x_{O,surface} + O^x_{O,surface} + 2h^\bullet \rightarrow (SO_4)^x_{O,surface} + V^{\bullet\bullet}_{O,surface} \quad (2)$$

This leads to the complete reaction:

$$SO_{2,gas} + 2O^x_{O,surface} + 2h^\bullet \rightarrow (SO_4)^x_{O,surface} + V^{\bullet\bullet}_{O,surface} \quad (3)$$

It should be noted here that the overall reduction of the defect electron concentration might lead to the observed first "resistance step". An additional positive charge on the grain surface forms, here denoted by $V^{\bullet\bullet}_{O,surface}$. It is compensated by a defect electron depleted space charge zone in the crystal. This could lead to a step-like resistance increase, when exposed to even small amounts of SO_2 in the gas. One could assume that an enhancement layer was present at the grain boundary before poisoning. This would make sense, since adsorbed oxygen at the grain boundary leads to a negative surface charge and hence an enhancement region in the p-type bulk follows. In this case, Eq. (3) describes how the enhancement is reduced.

According to Eq. (3), the amount of oxygen that is located at the grain boundary is reduced by this process. Therefore, one should expect that a low oxygen concentration in the gas promotes and a high oxygen concentration inhibits the formation of the sulfate phases. This is in good agreement with Fig. 3. The "first resistance step" is much faster in low-oxygen atmospheres. The decomposition, however, reflected by the longer time remains unchanged.

Such a surface reaction should not be limited to earth-alkaline containing perovskite. This agrees with results obtained on doped resistive $LaFeO_3$ sensors that were exposed to sulfur enriched O_2/N_2 mixtures. Here, fast but small resistance steps were also observed [15]. After this adsorption and sulfate forming process, all surface sites are occupied and the resistance should remain constant. That might be the case for temperatures lower than about 700°C.

At higher temperature, STF35 decomposes. Since besides $SrSO_4$ lines only cubic perovskite lines and pseudo brookite (Fe_2TiO_5) lines were found in the XRD patterns of poisoned sensors, a decomposition of STF35 acc. to Eq. (4) is assumed.

$$SrTi_{0.65}Fe_{0.35}O_{3-\delta} + nO_2 + \beta SO_2 \rightarrow \beta SrSO_4 + (1-\beta)SrTi_{\frac{1.95-\beta}{3(1-\beta)}}Fe_{\frac{1.05-2\beta}{3(1-\beta)}}O_{3-\delta'} + \frac{\beta}{3}Fe_2TiO_5 \quad (4)$$

β denotes the reaction progress. It is a measure for the amount of $SrSO_4$ and also for the amount Fe_2TiO_5 that has formed. Since per three formed $SrSO_4$ molecules only one Fe_2TiO_5 molecule has formed, it becomes clear, why Fe_2TiO_5 lines appear only very weakly in the XRD patterns of sulfur poisoned sensors.

The oxygen deficiency parameters of STF35 and the remaining perovskite, δ and δ', respectively, depend on the oxidation state of the iron. The amount of oxygen n that is necessary for Eq. (4) depends on δ, δ' and on β.

As a result of Eq. (4), an iron-depleted strontium titanate is formed. The reaction starts with $\beta = 0$ (= STF35) and reaches its end for $\beta = 0.525$. Then, the remaining perovskite is pure strontium titanate, which co-exists together with Fe_2TiO_5 and $SrSO_4$. With increasing reaction progress β one should measure mainly the conductivity of undoped $SrTiO_3$. In pure $SrTiO_3$ the conductivity is much lower than in STF35, it is strongly thermally activated and its slope in $SrTiO_3$ thick-film reaches only values of $m < 0.2$ [4]. This agrees very well with the observed results of sulfur oxide poisoned sensors [10].

5. Conclusion

Several tests investigating parameters that affect deterioration of temperature independent resistive oxygen sensor material STF35 were conducted. It turned out

that at low temperatures SO_2 adsorption and sulfate formation is likely. At higher temperatures, the material decomposes to strontium sulfate. As a conclusion, one should look for resistive oxygen sensitive materials that are earth alkaline-free, in order to get temperature independent and long-term stable sensors.

Notes.

1. For comparison: in real exhaust gas the concentration of sulfur dioxide due to sulfur components in the fuel is less than 10 ppm (conventional fuel with 200 mg/kg sulfur). So-called sulfur-free fuels contain less than 10 mg/kg fuel sulfur, leading to about 0.5 ppm SO_2 in the exhaust
2. The notation of Kröger & Vink is used [18]. To improve understandability, especially for readers that are not familiar with relative lattice charges, a conventional nomenclature is used in Fig. 6.

References

1. T.Y. Tien, H.L. Stadler, E.F. Gibbons, and P.J. Zacmanidis, *Ceram. Bull.*, **54**, 280 (1975).
2. A. Takami, *Ceram. Bull.*, **67**, 1956 (1988).
3. J. Gerblinger and H. Meixner, *J. Appl. Phys.*, **67**, 7453 (1990).
4. J. Gerblinger, M. Hauser, and H. Meixner, *J. Am. Ceram. Soc.*, **78**, 1451 (1995).
5. T.S. Stefanik and H.L. Tuller, *J. Eur. Ceram. Soc.*, **21**, 1967 (2001).
6. N. Izu, W. Shin, N. Murayama, and S. Kanzaki, *Sensors and Actuators B*, **93**, 449 (2003).
7. P.T. Moseley and D.E. Williams, *Polyhedron*, **8**, 1615 (1989).
8. D.E. Williams, B.C. Tofield, P. McGeehin, and Oxygen Sensors, European Patent Specification, EP 0062994 (1982).
9. R. Moos, W. Menesklou, H.-J. Schreiner, and K.H. Härdtl, *Sensors and Actuators B*, **67**, 178 (2000).
10. R. Moos, F. Rettig, and C. Plog, *Sensors and Actuators B,* **93**, 42 (2003).
11. H. Meixner, S. Kornely, D. Hahn, H. Leiderer, B. Lemire, and B. Hacker, Gas Sensor, *United States Patent Specification*, US 6,101,865 (1995)
12. F. Rettig, R. Moos, and C. Plog, *Sensors and Actuators B*, **93**, 36 (2003).
13. L. Wan, "*Poisoning of perovskite oxides by sulfur dioxide*," in *Properties and Applications of Perovskite-Type Oxides*, edited by L.G. Tejuca, and J.L.G. Fierro (Marcel Dekker Inc., New York, USA 1993) p. 145ff.
14. T. Schulte, R. Waser, E.W.J. Römer, H.J.M. Bouwmeester, U. Nigge, and H.-D. Wiemhöfer, *J. Eur. Ceram. Soc.*, **21**, 1971 (2001).
15. F. Rettig, R. Moos, and C. Plog, "Novel temperature independent resistive oxygen sensor without sulfur instability for combustion engine exhausts," Sensor 2003, in *Proceedings of the 11th International Conference*, Nürnberg, Germany, 13–15. May 2003, pp. 277–282.
16. A. Müller and K.H. Härdtl, *Appl. Phys. A*, **49**, 75 (1989).
17. C. Tragut and K.H. Härdtl, *Sensors and Actuators B*, **4**, 425 (1991).
18. F.A. Kröger and H.J. Vink, "Relations between the Concentrations of Imperfections in Crystalline Solids," in, *Solid State Physics*, edited by F. Seitz, and D. Turnbull (Academic Press, New York, 1956), Vol. 3, pp. 307–435.